Supporting Information

Navigating fast and uniform zinc deposition via a versatile metal-organic complex interphase

Huanyan Liu, Jian-Gan Wang*, Wei Hua, Lingbo Ren, Huanhuan Sun, Zhidong Hou,

Yu Huyan, Yunjing Cao, Chunguang Wei, Feiyu Kang*

Experimental Section

Synthesis of Zn-PA coated Zn anode (Zn-PA@Zn): Firstly, 30 μL of 70% phytic acid (PA) was injected to 30 ml of 2 to 1 mixed solution of deionized (DI) water and ethanol. After stirring for 5 min, the solution was transferred into a glass culture dish. Then, Zn plates with a diameter of 12 mm were putted into the solution and stand for several minutes. Zn-PA@Zn was obtained after being alternatively washed with DI water and ethanol. Ba-PA, Al-PA, and Sn-PA coordinated Zn anodes were prepared using the same procedure except for the adding of 30 mg of $BaCl_2$, $Al_2(SO_4)_3$, and $SnCl_4$, respectively. Sn-Tannin (TA) coordinated Zn anode was prepared using the same procedure except for the change of PA to TA.

Synthesis of MnO$_2$: In a typical procedure, 2 mM of $KMnO_4$ was dissolved in 50 mL of DI water under magnetic stirring for 15 min. Subsequently, 5 mL of 2 M H_2SO_4 was added into the above solution. After stirring for another 15 min, 3 mM of Zn powders were added into the mixture. The reaction lasted for 2 h under continuous magnetic stirring at room temperature. Finally, the resulting precipitate was collected and washed with DI water and ethanol alternatively for three times. MnO_2 powders were obtained after being dried in an oven at 80 °C for 12 h.

Assembly of Zn/Zn symmetric cells and Zn/MnO$_2$ cells: CR2025-type coin symmetric cells were assembled with identical electrodes of bare Zn or Zn-PA@Zn (diameter: 12 mm, thickness: 80 μm), 2 M $ZnSO_4$ electrolyte and glass fiber separators. Zn‖MnO$_2$ full cells were assembled by using pure Zn or Zn-PA@Zn as anodes, 2 M $ZnSO_4$ as electrolyte and glass fiber as separators. All batteries were assembled in open air

conditions and aged for 12 hours before electrochemical measurements.

Materials characterization: The physical morphology was characterized by scanning electron microscopy (SEM, NanoSEM 450, FEI). X-ray diffractometer (XRD, X'Pert PRO MPD, Philips) was carried out to confirm the crystallographic structure of the products using Cu-Kα as the radiation source (λ= 1.5418 Å). The surface wettability of anodes was performed by OCA25 contact angle measuring system (Dataphysics, Germany). Fourier transform infrared (FTIR, ThermoNicolet iS50) and X-ray photoelectron spectroscopy (XPS, ESCALAB 250Xi, Thermo Scientific) were employed to analyze the element and surface chemistry of the samples.

Electrochemical measurement: The cycling and rate performance were measured on the Land Battery Testing System at room temperature. Solartron electrochemical workstation (1400 + 1470E, England) was employed to collect the cyclic voltammetry (CV), electrochemical impedance spectra (EIS), linear sweep voltammetry (LSV), and linear polarization curves. Specifically, CV curves were measured at a scan rate of 0.1 mV s^{-1} and EIS plots were tested in the frequency ranging from 100 kHz to 10 mHz with a perturbation amplitude of 5 mV. LSV and linear polarization curves were collected at the voltage range of -1.1 ~ -1.85 V and -1.1 ~ -0.95 V, respectively, with scan rate of 5 mV s^{-1}.

Simulation of the Electric Field Contribution: A simplified 2D electrodeposition model based on COMSOL was established to compare the proportional schematics of electric field distribution during cycling. The length of the entire model was set to 8 μm. The protuberance of Zn surface was represented by three semicircles with a

diameter of 1 μm and a height of 1 μm. In addition, there was a Zn-PA layer with a thickness of 1 μm for Zn-PA@Zn electrodes on the basis of primary model. It was reported that the ionic conductivity of 2 M $ZnSO_4$ electrolyte was ≈5 S m^{-1}.[1] The overpotential of 500 mV was employed as voltage excitation between the anode side and the electrolyte side.
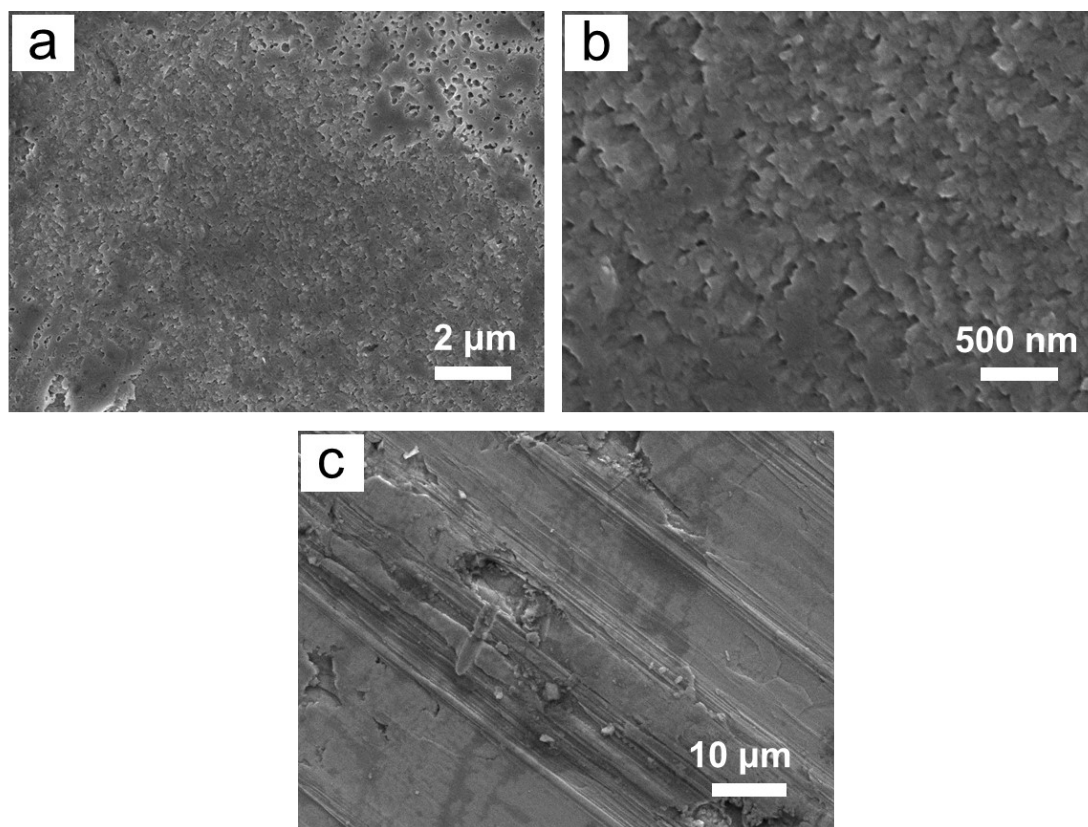
Fig. S1 Top-view SEM images of (a, b) Zn-PA@Zn and (c) bare Zn anode.
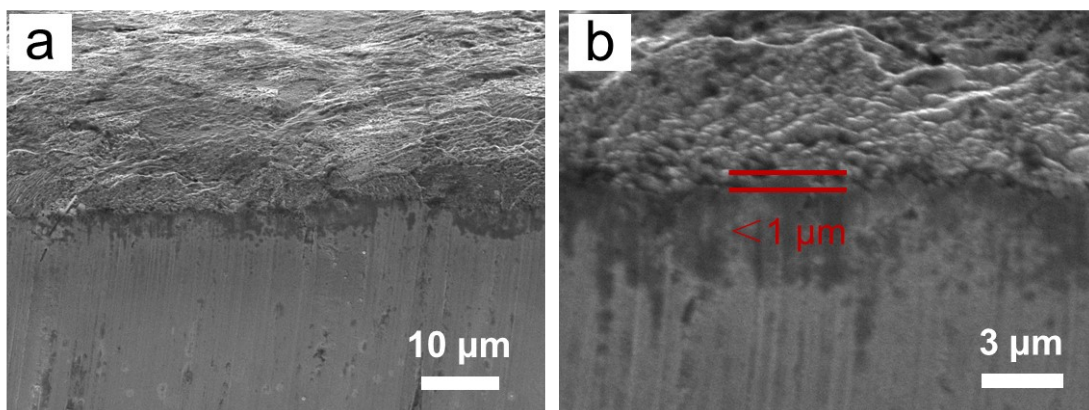
Fig. S2 Cross-section SEM images of Zn-PA@Zn.
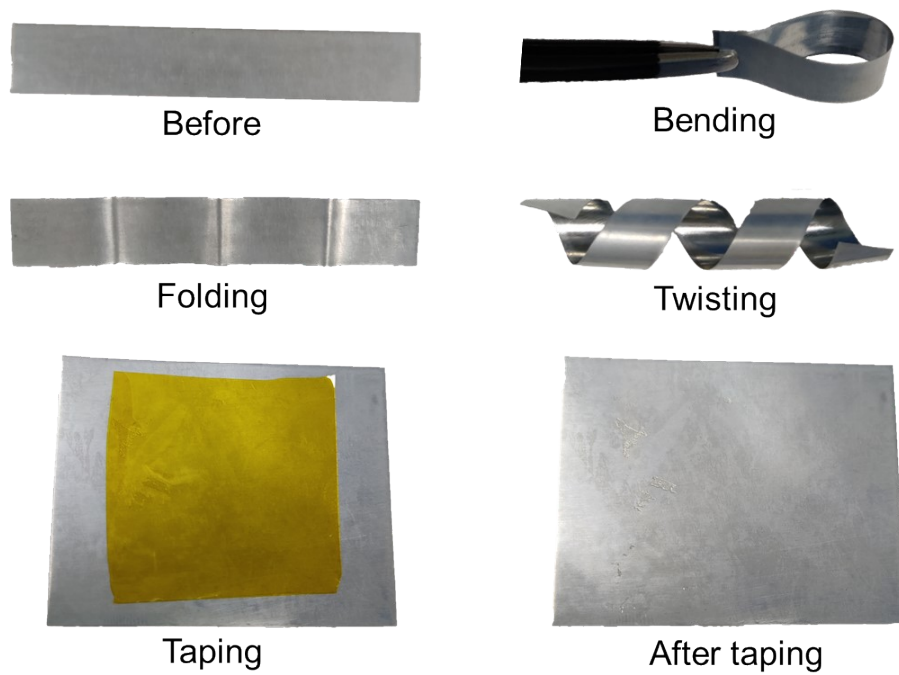
Fig. S3 Optical images of Zn-PA@Zn anode under bending, folding, twisting, and even taping states.

Fig. S4 Optical image of the scale-up Zn-PA@Zn electrode.
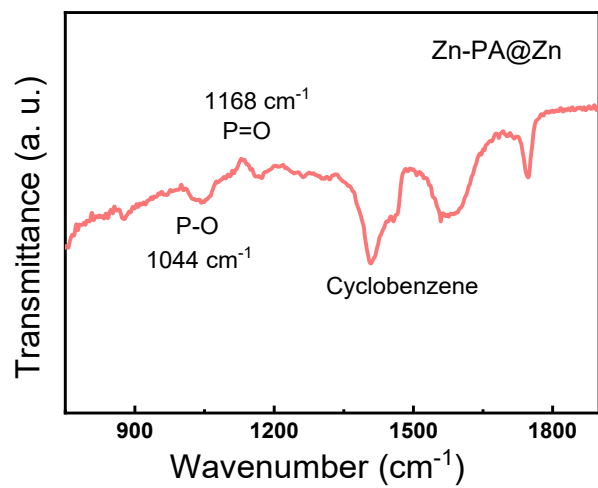
Fig. S5 Fourier transform infrared (FTIR) curve of Zn-PA@Zn electrode.
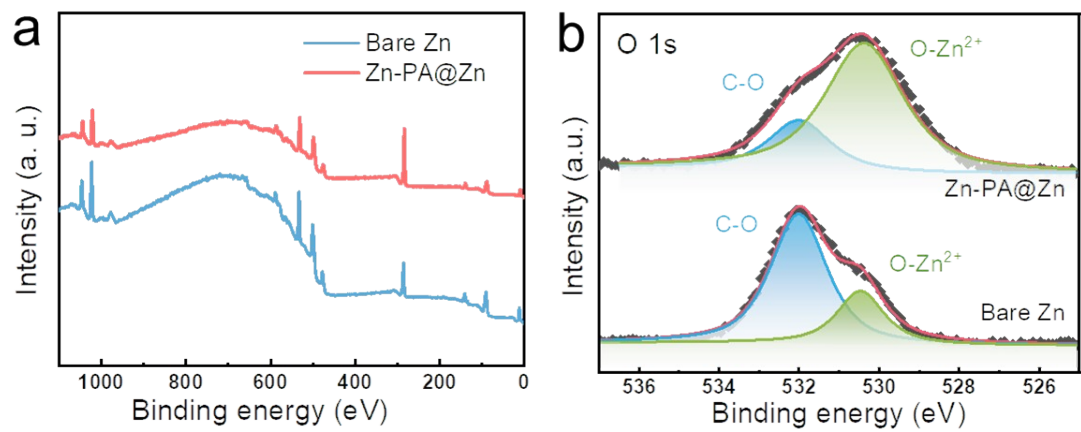
Fig. S6 (a) Survey XPS profiles and (b) high-resolution O 1s XPS patterns of bare Zn and Zn-PA@Zn electrodes.
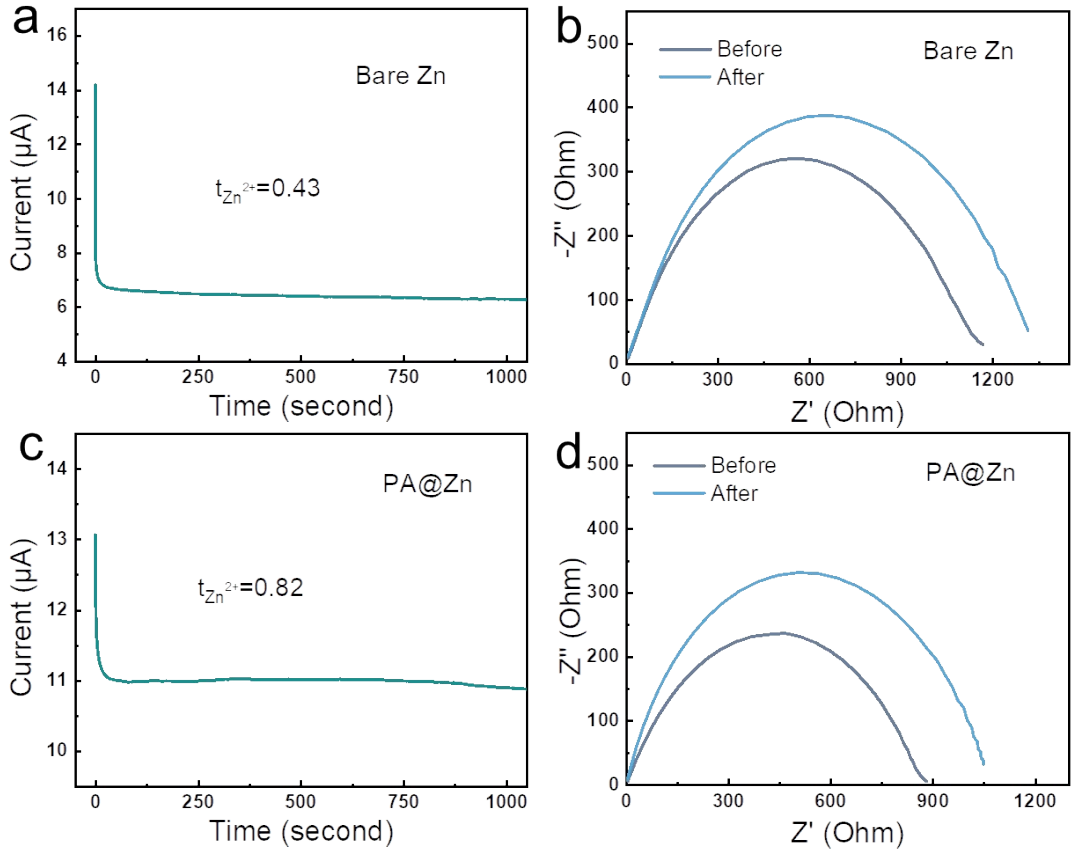
Fig. S7 Current variation with time during polarization and the associated EIS curves of (a, b) bare

Zn and (c, d) Zn-PA@Zn symmetrical cells with applied potential difference of 15 mV.

The Zn^{2+} transference number (t_{Zn2+}) was calculated according to the Bruce-

Vincent method:

$$t_{Zn^{2+}} = \frac{I_s(V - I_0 R_0)}{I_0(V - I_s R_s)}$$

(1)

Where V is the applied potential (15 mV); I_0 and R_0 are the initial current and

interface resistance, respectively; I_s and R_s represent the steady-state current and

interface resistance, respectively. Therefore, the $t_{Zn^{2+}}$ value in Zn-PA@Zn system can

be calculated to 0.82, whereas the value in bare Zn system is only 0.43.
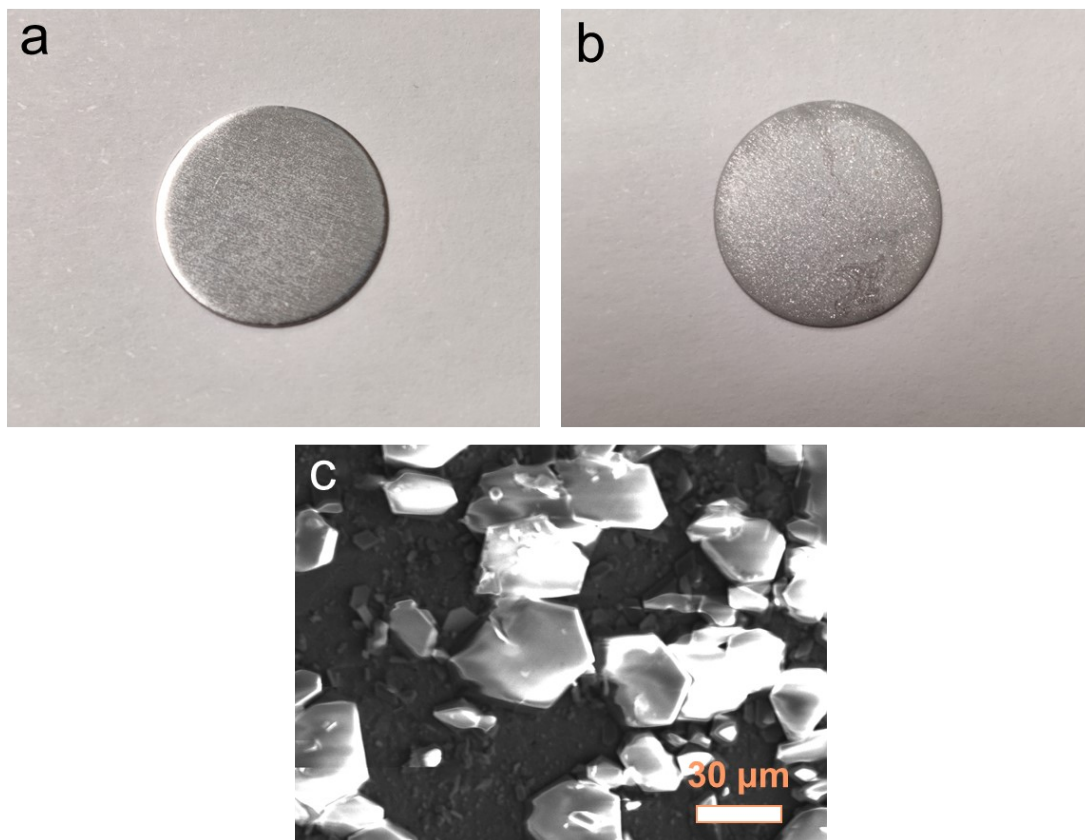
Fig. S8 Optical images of bare Zn (a) before and (b) after immersing in 2 M ZnSO$_4$ for 10 days. (c)

Magnified SEM image of bare Zn after immersing in 2 M ZnSO$_4$ for 10 days.
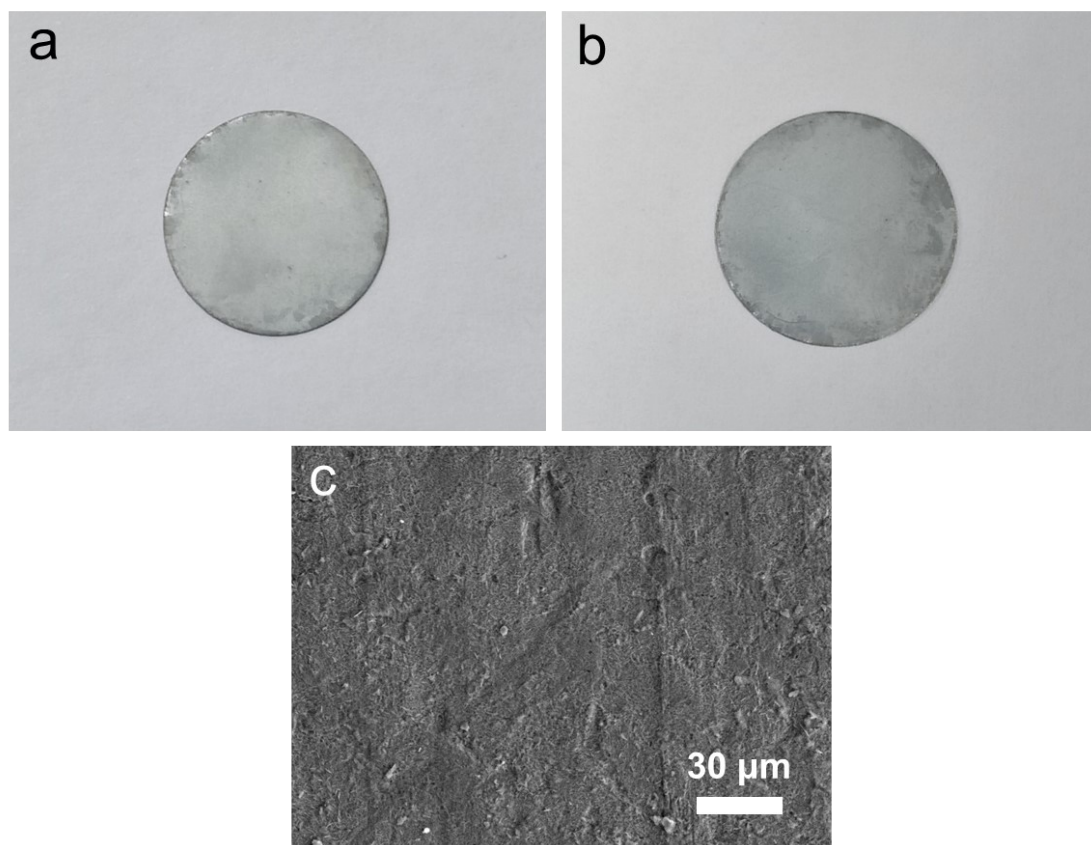
Fig. S9 Optical images of Zn-PA@Zn (a) before and (b) after immersing in 2 M ZnSO$_4$ for 10

days. (c) Magnified SEM image of Zn-PA@Zn after immersing in 2 M ZnSO$_4$ for 10 days.
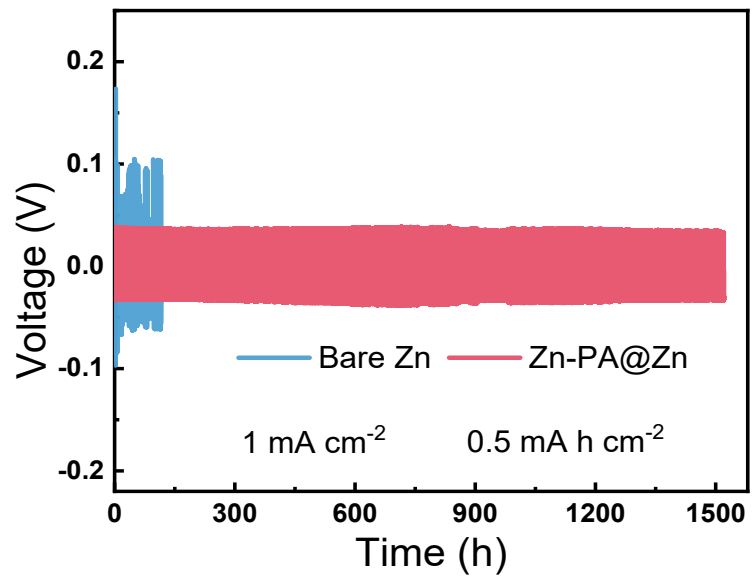
Fig. S10 Cycling performance of bare Zn and Zn-PA@Zn symmetric cells at 1 mA cm^{-2}.
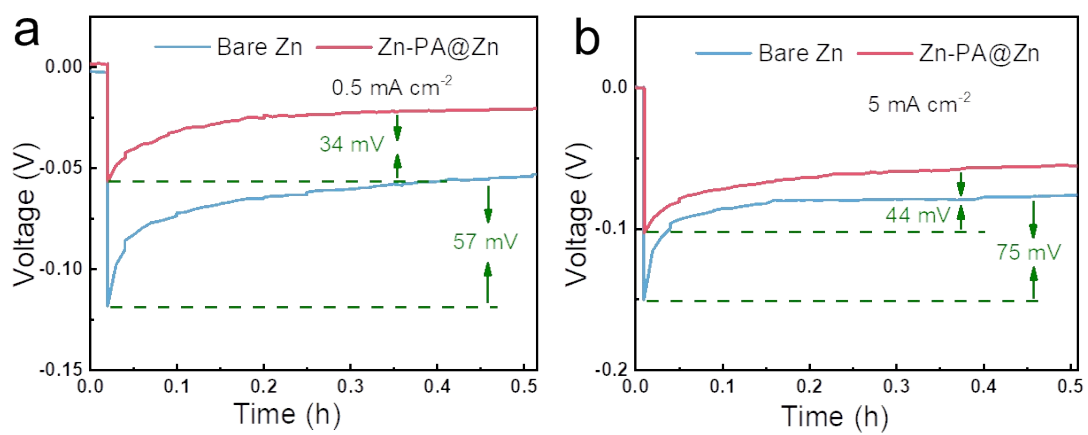
Fig. S11 Nucleation overpotential of bare Zn and Zn-PA@Zn symmetric cells at (a) 0.5 mA cm^{-2}

and (b) 5 mA cm^{-2}.
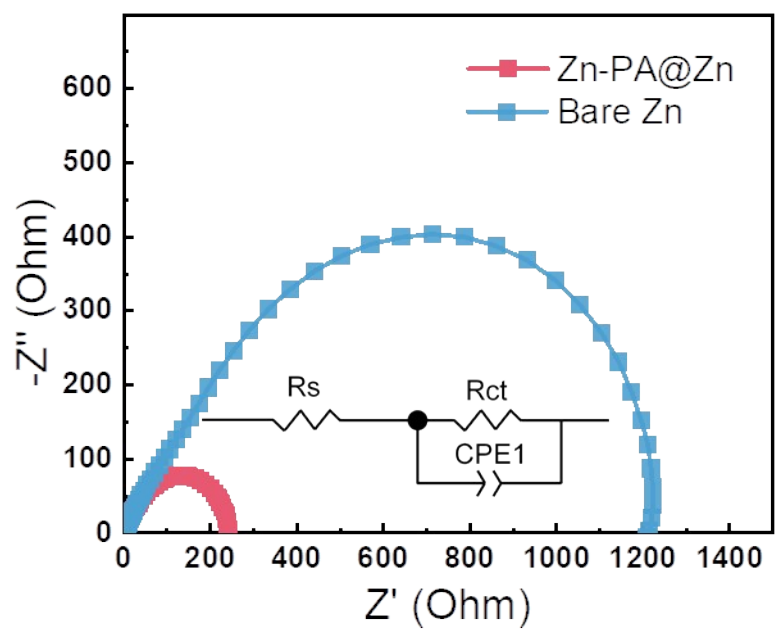
Fig. S12 EIS curves of the Zn-PA@Zn and bare Zn symmetric cells.
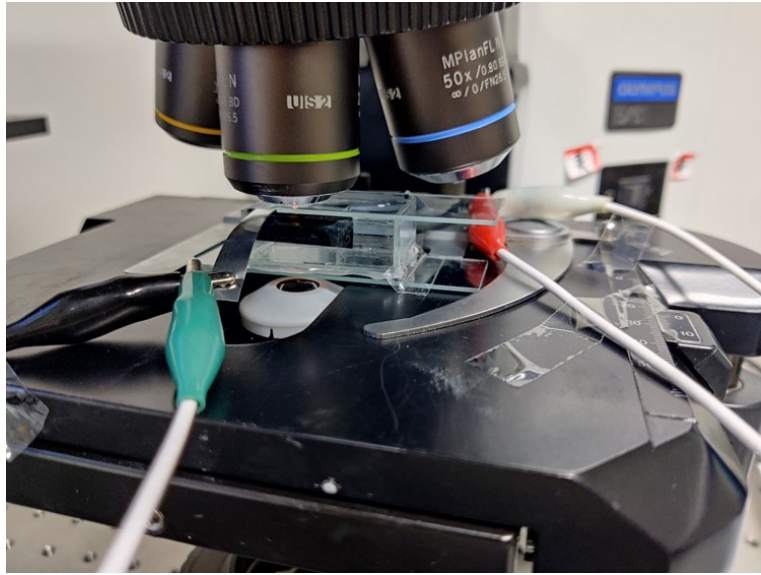
Fig. S13 Self-made symmetric cell model for in-situ optical microscope.
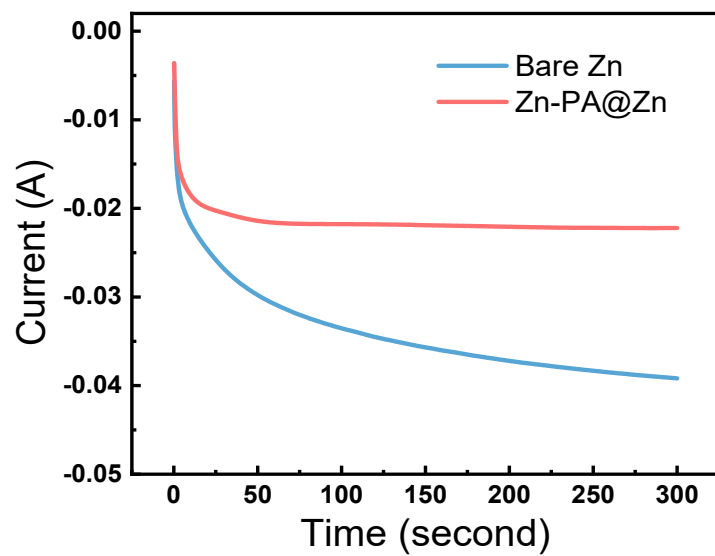
Fig. S14 Chronoamperometry curves of bare Zn and Zn-PA@Zn at an overpotential of -150 mV.
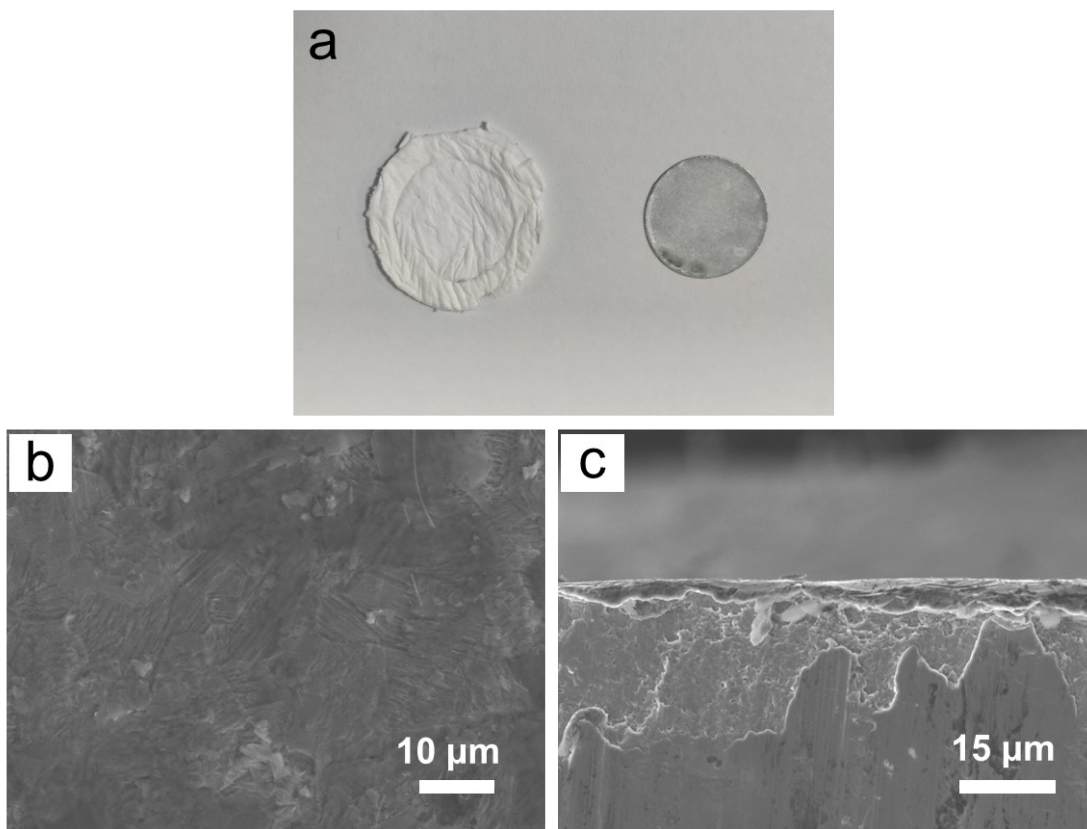
Fig. S15 (a) Detached Zn-PA@Zn cell after 50 cycles at 1 mA cm^{-2} and 0.5 mAh cm^{-2}. (b) Top-view, and (c) cross-section SEM images of Zn-PA@Zn.
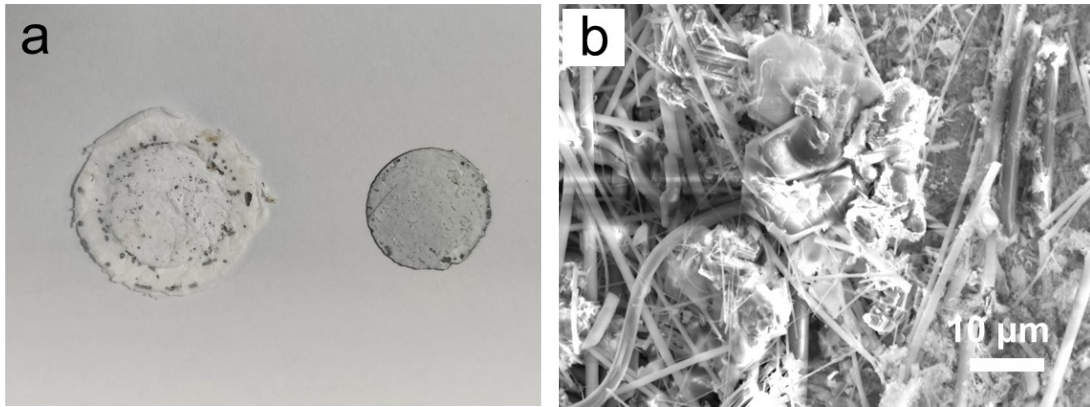
Fig. S16 (a) Detached bare Zn cell after 50 cycles at 1 mA cm^{-2} and 0.5 mAh cm^{-2}. (b) SEM image of bare Zn electrode after cycling.
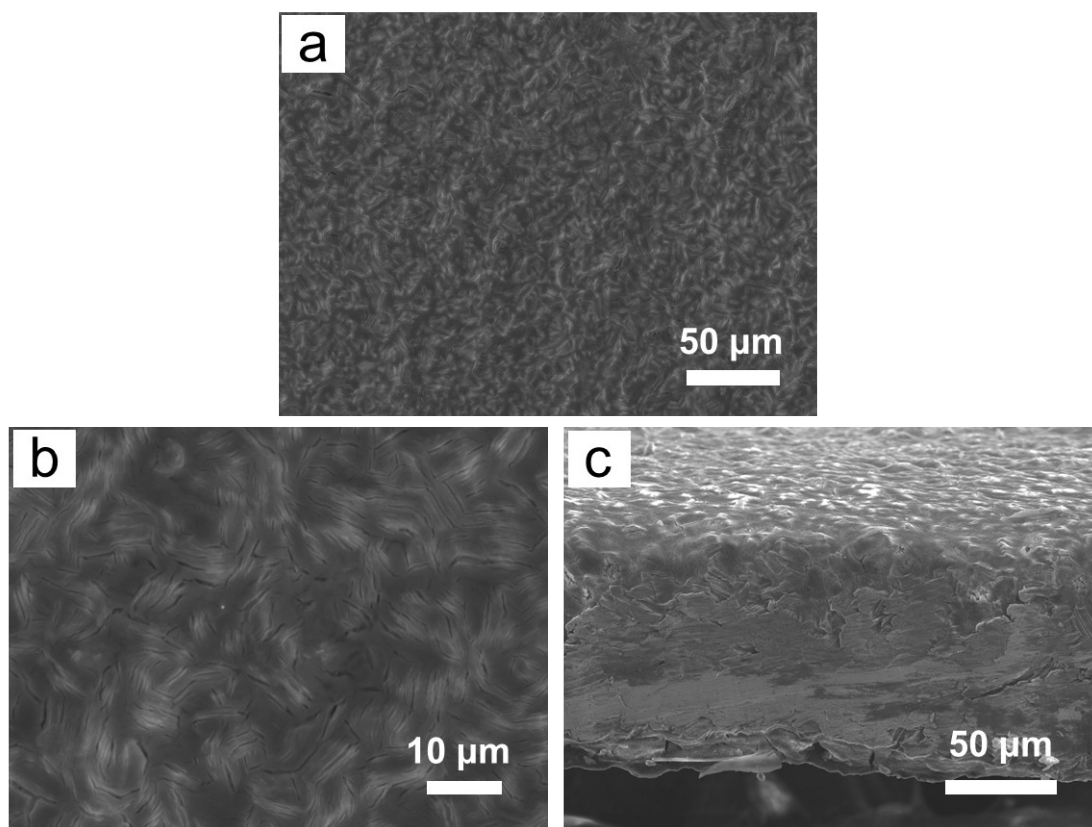
Fig. S17 (a, b) Top-view, and (c) cross-section SEM images of Zn-PA@Zn after plating for 10 mAh cm^{-2} at 10 mA cm^{-2}.
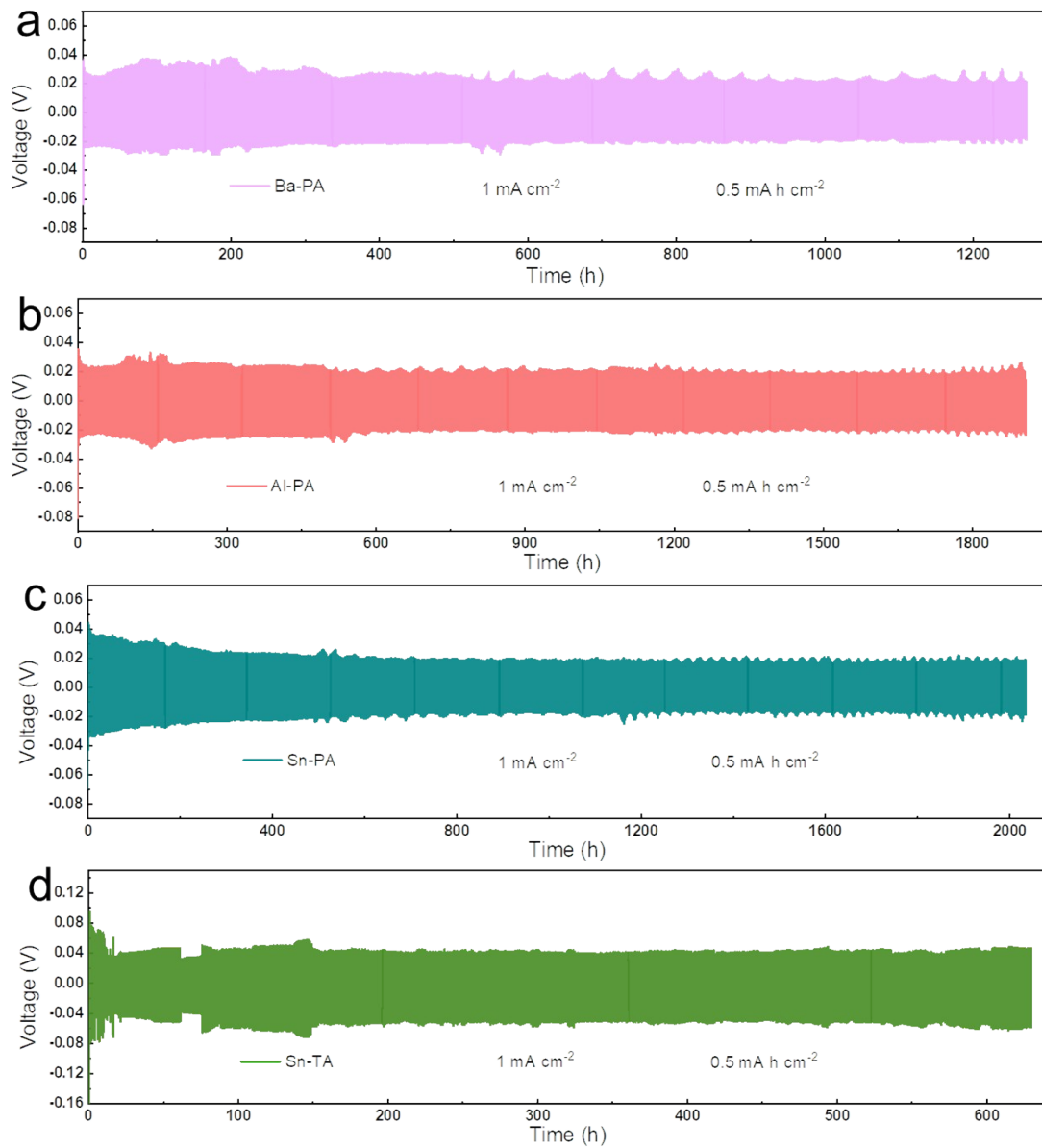
Fig. S18 Cycling performance of the as-prepared (a) Ba-PA@Zn, (b) Al-PA@Zn, (c) Sn-PA@Zn, and Sn-TA@Zn symmetric cells at 1 mA cm^{-2}.
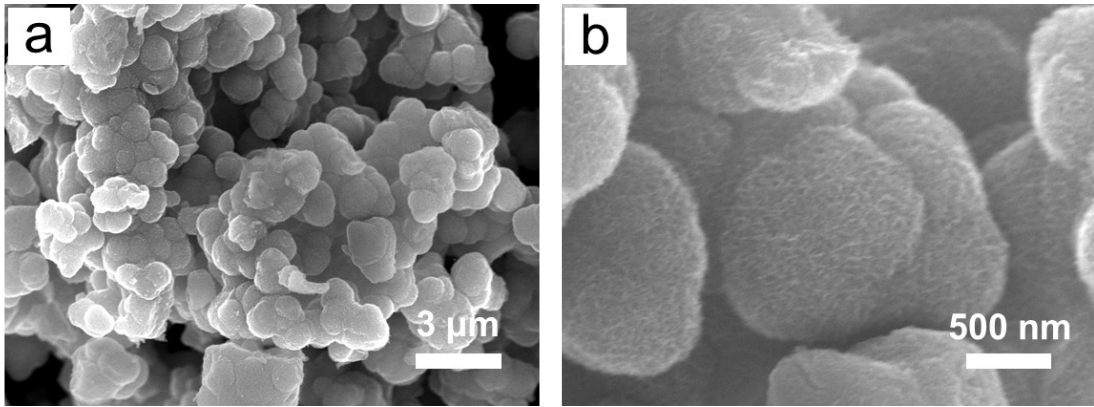
Fig. S19 SEM images of the MnO$_2$ sample.
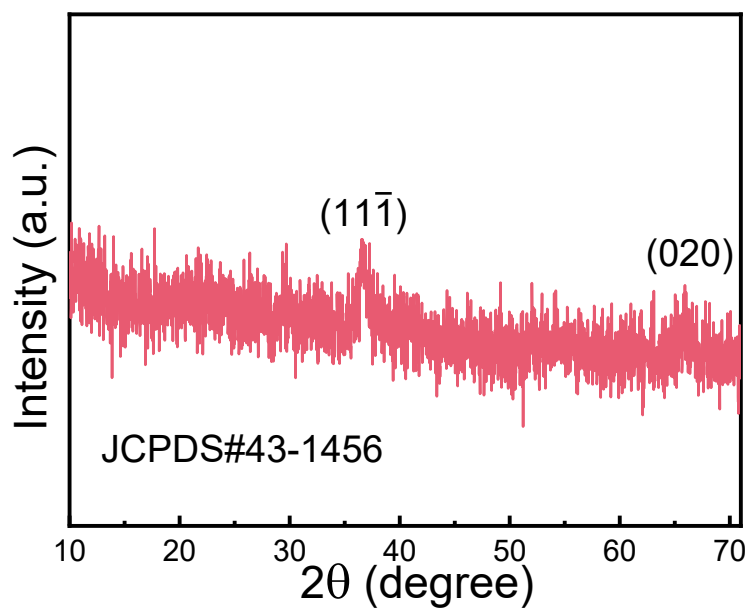
Fig. S20 XRD pattern of the as-prepared MnO$_2$.
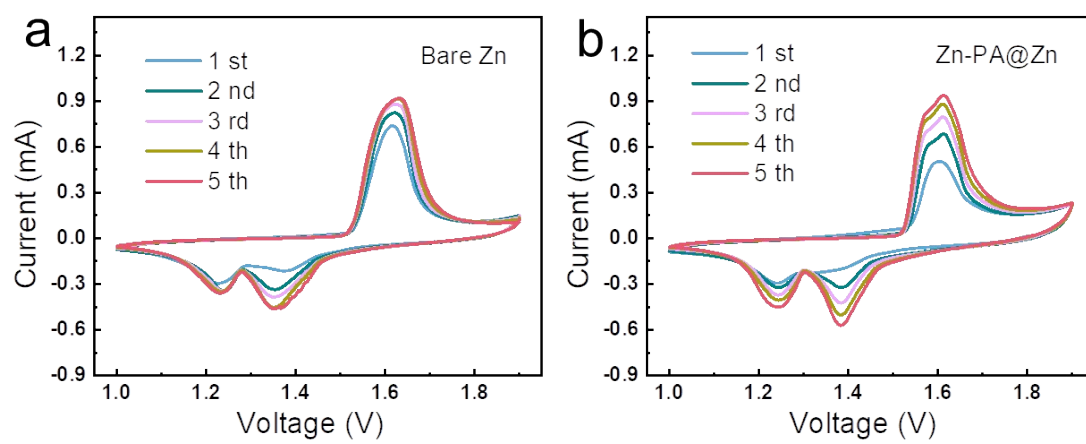
Fig. S21 CV curves of (a) bare Zn||MnO$_2$ and (b) Zn-PA@Zn||MnO$_2$ cells at a scan rate of 0.1 mV s^{-1}.
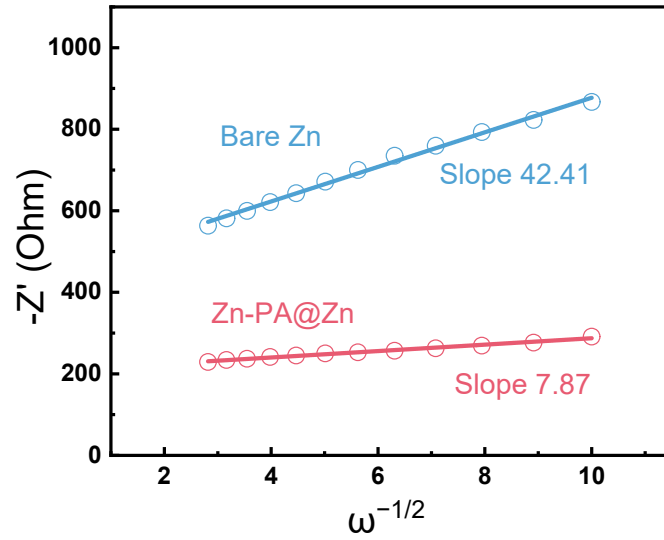
Fig. S22 Z'~ω$^{-1/2}$ fitting curves of the full cells based on EIS results.

The Zn^{2+} diffusion coefficient (D) was calculated according to $D=0.5R^2T^2n^{-4}F^{-4}A^{-2}C^{-2}\sigma^{-2}$. Here, R is the gas constant, T is the room temperature, n is the transfer number of the electrons during the Zn^{2+} reaction, F is the Faraday constant, A is the surface area of the electrode, C is the concentration of Li$^+$, σ is the slope obtained from the Z'~ω$^{-1/2}$ line. Thus the D value of Zn-PA@Zn||MnO$_2$ cell was calculated to be 6.99×10^{-10} cm^2 s^{-1}, whereas the value for bare Zn||MnO$_2$ cell was 2.41×10^{-11} cm^2 s^{-1}.
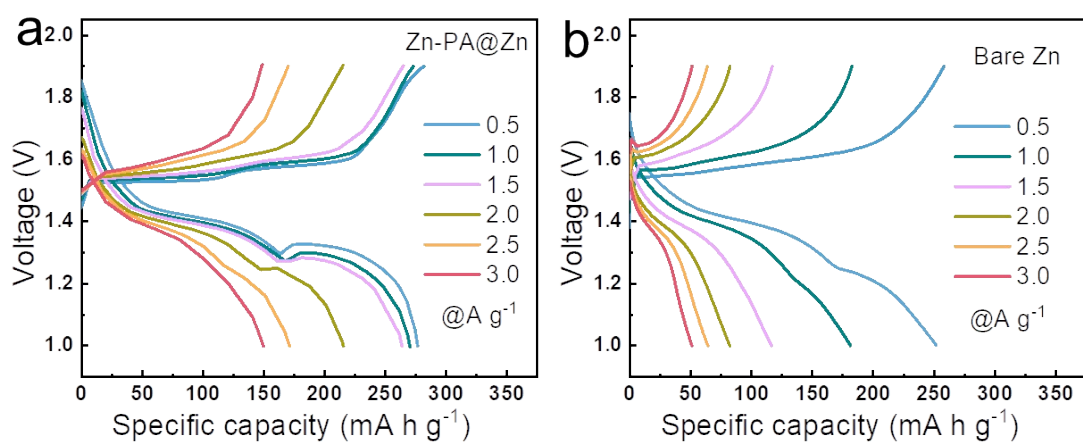
Fig. S23 Charge-discharge profiles of (a) Zn-PA@Zn‖MnO_2 and (b) bare Zn‖MnO_2 cells at

different current densities.
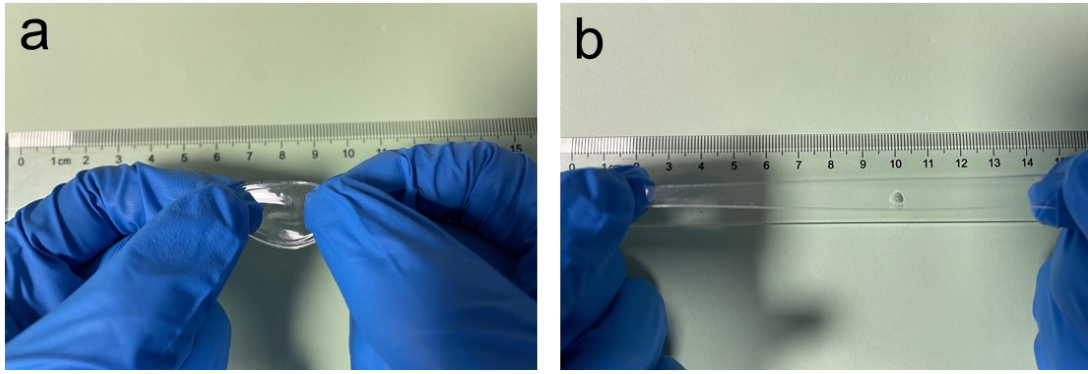
Fig. S24 Digital photos of the elastic PAM gel electrolyte, showing the splendid elasticity.
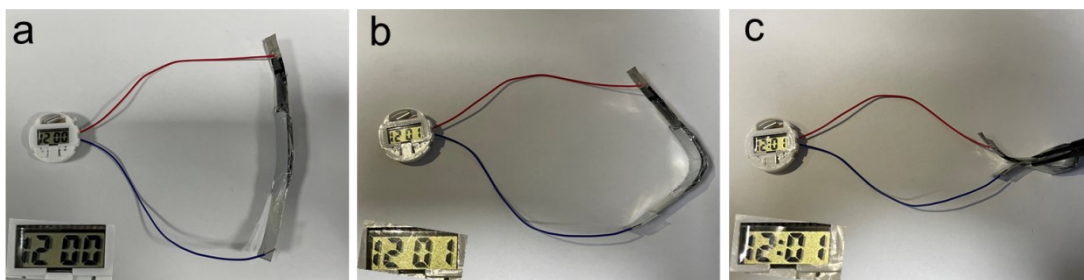
Fig. S25 Digital photos of a ZIB cell powering an electronic watchband under (a) flat, (b) bending 90º and (c) bending 180º conditions.

Fig. S26 LED display screen before connection with the ZIB cells.

Table S1 The comparison of CPC and average CE with other reported literatures.

Electrode or electrolyte	Current density (mA cm^{-2})	Average CE (%)	CPC (mAh cm^{-2})	Reference
Zn-PA@Zn	2	99.9	800	This work
ZnO-3D@Zn	2	99.5	150	[2]
ZnS@Zn	2	99.2	200	[3]
Zn(ClO$_4$)$_2$·6H$_2$O electrolyte	0.5	98.4	45	[4]
Zn(TFSI)$_2$-TFEP@MOF@Zn	0.5	99.9	175	[5]
Antisolvents	1	99.7	450	[6]
Glucose Additive	1	97.2	100	[7]
CNG@Zn	0.5	99.4	150	[8]

Table S2 The CPC comparison of Zn-PA@Zn symmetric cell with other reported literature.

Electrode or electrolyte	Current density $(mA\ cm^{-2})$	Areal capacity per cycle $(mAh\ cm^{-2})$	CPC $(Ah\ cm^{-2})$	Reference
Zn-PA@Zn	5	1.25	1.25	This work
ZnO-3D@Zn	5	1.25	1.25	[2]
TiO_2@Zn	2	2	0.28	[9]
Kaolin@Zn	4.4	1.1	1.76	[10]
Polyamide@Zn	0.5	0.25	2	[11]
ZnS@Zn	2	2	1.1	[3]
CNG@Zn	1	0.5	1.5	[8]
$Zn(OTF)_2$-$Zn(NO_3)_2$ electrolyte	0.5	0.5	0.3	[12]
Polyimide@Zn	4	2	1.7	[13]
$Zn_3(PO_4)_2$@Zn	0.5	99.4	150	[14]

References

1. Y. Zeng, X. Zhang, R. Qin, X. Liu, P. Fang, D. Zheng, Y. Tong and X. Lu, *Adv. Mater.*, 2019, **31**, 1903675.

2. X. Xie, S. Liang, J. Gao, S. Guo, J. Guo, C. Wang, G. Xu, X. Wu, G. Chen and J. Zhou, *Energy Environ. Sci.*, 2020, **13**, 503-510.

3. J. Hao, B. Li, X. Li, X. Zeng, S. Zhang, F. Yang, S. Liu, D. Li, C. Wu and Z. Guo, *Adv. Mater.*, 2020, **32**, 2003021.

4. W. Yang, X. Du, J. Zhao, Z. Chen, J. Li, J. Xie, Y. Zhang, Z. Cui, Q. Kong, Z. Zhao, C. Wang, Q. Zhang and G. Cui, *Joule*, 2020, **4**, 1557-1574.

5. L. Cao, D. Li, T. Deng, Q. Li and C. Wang, *Angew. Chem. Int. Ed.*, 2020, **59**, 19292-19296.

6. J. Hao, L. Yuan, C. Ye, D. Chao, K. Davey, Z. Guo and S. Z. Qiao, *Angew. Chem. Int. Ed.*, 2021, **60**, 7366-7375.

7. P. Sun, L. Ma, W. Zhou, M. Qiu, Z. Wang, D. Chao and W. Mai, *Angew. Chem. Int. Ed.*, 2021, **60**, 18247-18255.

8. X. Zhang, J. Li, D. Liu, M. Liu, T. Zhou, K. Qi, L. Shi, Y. Zhu and Y. Qian, *Energy Environ. Sci.*, 2021, **14**, 3120-3129

9. Q. Zhang, J. Luan, X. Huang, Q. Wang, D. Sun, Y. Tang, X. Ji and H. Wang, *Nat. Commun.*, 2020, **11**, 3961.

10. C. Deng, X. Xie, J. Han, Y. Tang, J. Gao, C. Liu, X. Shi, J. Zhou and S. Liang, *Adv. Funct. Mater.*, 2020, **30**, 2000599.

11. Z. Zhao, J. Zhao, Z. Hu, J. Li, J. Li, Y. Zhang, C. Wang and G. Cui, *Energy Environ. Sci.*, 2019, **12**, 1938-1949.

12. D. Li, L. Cao, T. Deng, S. Liu and C. Wang, *Angew. Chem. Int. Ed.*, 2021, **60**, 13035-13041.

13. M. Zhu, J. Hu, Q. Lu, H. Dong, D. D. Karnaushenko, C. Becker, D. Karnaushenko, Y. Li, H. Tang, Z. Qu, J. Ge and O. G. Schmidt, *Adv. Mater.*, 2021, **33**, 2007497.

14. X. Zeng, J. Mao, J. Hao, J. Liu, S. Liu, Z. Wang, Y. Wang, S. Zhang, T. Zheng, J. Liu, P. Rao and Z. Guo, *Adv. Mater.*, 2021, **33**, 2007416.